A Combined Field Approach to Scattering from Infinite Elliptical Cylinders Using the Method of Ordered Multiple Interactions

Robert J. Adams, *Student Member, IEEE,* and Gary S. Brown, *Fellow, IEEE*

***Abstract*— The method of ordered multiple interactions (MOMI) is an iterative procedure which has been demonstrated to provide a rapidly convergent series for the problem of wave scattering from perfectly conducting surfaces rough in a single dimension. In this paper, we consider the extension of this technique to the problem of scattering from infinite elliptical cylinders. For an incident plane wave having its electric field polarized along the axis of the cylinder a combined field formulation of the scattering problem is found to provide a rapidly convergent MOMI series. The determination of an optimal combined field representation for the scattering problem in this case is also discussed. An extension of the MOMI method is necessary to properly treat the remaining polarization.**

***Index Terms*— Electromagnetic scattering, elliptic cylinders, multiple interactions.**

I. Introduction

An important goal of electromagnetic analysis is the development of efficient numerical schemes which are applicable to a wide range of problems. One important class of such techniques is the boundary integral equation method for time harmonic fields [1], [2]. The use of a moment method procedure reduces this integral equation formulation to a finite-dimensional matrix equation of the form $Ax = b$ where A is a dense matrix [3]. Straightforward inversion of this system is often computationally prohibitive for realistically sized problems.

A widely employed alternative to this direct method of solution is the use of an iterative approach for which the computational complexity scales as

$$T \sim cn_iN^\sigma \tag{1}$$

where n_i is the number of iterations required to achieve a given accuracy, σ is a constant which depends on the method of solution and c is a method and implementation dependent constant. The method of ordered multiple interactions (MOMI) discussed herein provides a physically based approach which can significantly reduce n_i relative to other iterative techniques which are based on a mathematical minimization procedure (e.g., [4], [5]). Although MOMI can be used with techniques which reduce the cost of a matrix–vector multiply and thereby reduce σ [6], in the following, we perform all such computations in the standard manner such that $\sigma = 2$.

MOMI was originally developed as an iterative method for solving the magnetic field integral equation (MFIE) encountered in scattering from extended perfect electric conductors (PEC's) rough in one dimension [7]. The convergence properties of the MOMI series for this problem were found to be excellent. This success has led to an investigation of the conditions under which the method can be used to obtain a rapidly convergent series solution to the problem of scattering from closed PEC surfaces [8].

Strictly speaking, the MFIE applies only to closed PEC surfaces [9]. However, in analyzing scattering from extended rough surfaces some type of tapered incident field is typically used such that the illuminated surface area is a small fraction of the total surface area. This effectively results in an open-surface scattering problem. In investigating the application of MOMI to closed surfaces we are considering cases in which it is not possible to determine *a priori* that the currents over a significant portion of the surface are zero and, thereby, truncate the interaction domain. In all cases we are considering, the support of the illumination is much larger than the support of the cylinder.

Other authors have discussed similar approaches to the closed body scattering problem [10], [11]. Of particular interest to this study is the conclusion that the MOMI series for the MFIE does not converge for scattering from cylinders [10]. In the following, it is demonstrated that while true in many cases, this conclusion is not correct in general. We further show that the convergence difficulties observed in [10] are ameliorated when a well-behaved formulation of the scattering problem is used. It is anticipated that a similar formulation will also remove the convergence difficulties encountered in [11] for closed body scatterers.

II. Summary of Results

To simplify the present investigation, we have limited our consideration to scattering from elliptical cylinders of infinite extent for which the three-dimensional vector electromagnetic problem reduces to a two-dimensional (2-D) scalar problem. The geometric and polarization definitions which will be used throughout are illustrated in Fig. 1. The infinite axis of the cylinder is taken to be coincident with the y axis of the

Manuscript received February 23, 1998; revised September 11, 1998. This work was supported by the Air Force Office of Scientific Research, Air Force Materials Command, USAF, under Grant F49620-96-1-0039.

The authors are with the Bradley Department of Electrical and Computer Engineering, Virginia Tech, Blacksburg, VA 24061 USA.

Publisher Item Identifier S 0018-926X(99)03719-9.

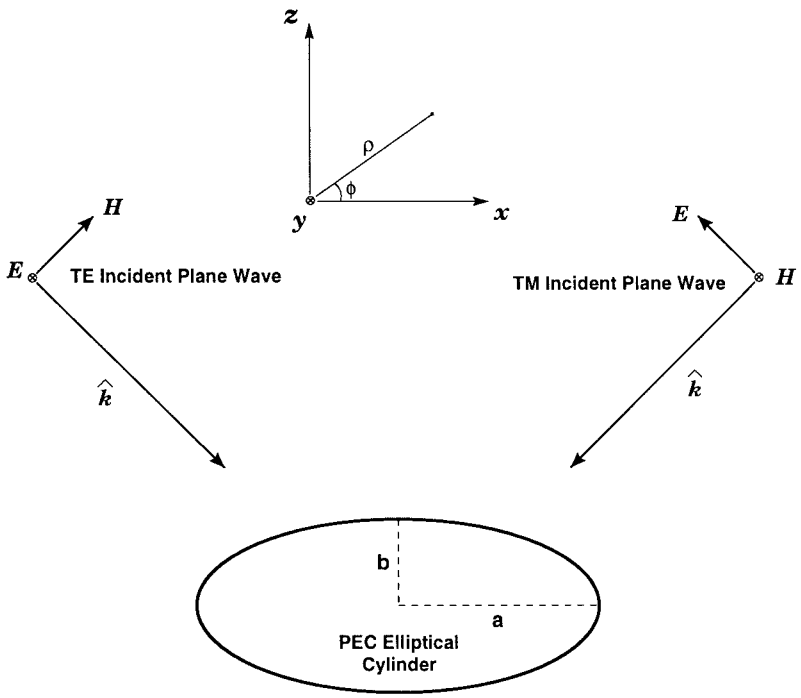

Fig. 1. Problem geometry and polarization definitions. The y axis of the Cartesian system is chosen to coincide with the axis of the ellipse. The ellipse's semi-major and semi-minor axes are, respectively, denoted by a and b. The TM- and TE-polarization designations specify which field component is transverse to the plane of incidence (the x-z plane).

Cartesian system. The cylinder's cross section is an ellipse defined by its semi-major and semi-minor axis lengths denoted, respectively, by a and b. The axial ratio of the cylinder is a/b. The relationship between the polar coordinate system defined by the pair (ρ, ϕ) to the Cartesian system is also shown. The TM- and TE-polarization designations in Fig. 1 specify which field component is transverse to the plane of incidence (the x-z plane). Thus, a TE-polarized field has its electric field parallel to the y axis. For all cases considered in this paper the incident field is a plane wave of unit amplitude traveling in the $-\hat{\mathbf{z}}$ direction. The convergence properties observed for this choice of incident field are representative of those obtained for an arbitrary incident field.

As discussed below, in applying MOMI to elliptical cylinders the question arises as to how the surface current unknowns should be organized in the matrix equation. Different orderings of the unknowns lead to MOMI series that incorporate different multiple scattering interactions in each iterate. In this paper, we consider the two different ordering schemes illustrated in Fig. 2. An ordering which is sequential-in-ϕ (SIP) mimics the progression of creeping waves around the cylinder, while the sequential-in-x (SIX) scheme is analogous to the forward/backward ordering used in [7] for rough surfaces.

Figs. 3 and 4 show the normalized residual error of the MOMI series for the MFIE formulation of the problem of TE and TM scattering from circular cylinders. The convergence properties are illustrated for cylinders of various radii using both the SIP and SIX ordering schemes. From these figures it is clear that the MOMI series solution of the MFIE formulation of the cylindrical scattering problem is not nearly as robust as the corresponding series solution of the rough-surface scattering problem.

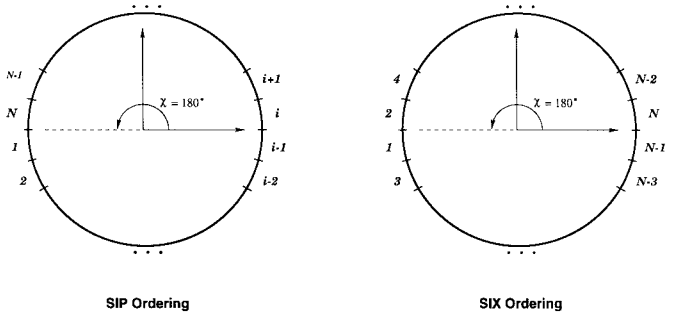

Fig. 2. Definition of SIP and SIX unknown orderings. For the SIP ordering the coefficients of the surface current basis functions are ordered sequentially-in-ϕ in the unknown vector ψ of (9). In the SIX approach the unknown coefficients are placed in ψ in the order in which they occur along an arbitrary line in the x-z plane. In both cases, the first element of ψ is specified by the central angle χ, which is measured counter clockwise from the x axis.

These poor convergence properties are somewhat surprising given the multiple scattering interpretation of the MOMI series in [7]. As discussed further below, this behavior results because MOMI attempts to approximate the integral operator of the closed body problem with a decoupled multiple scattering formulation. At and near the resonance points of the interior problem, this corresponds to the approximation of a singular or nearly singular operator with an operator which is well behaved in all cases.

This understanding suggests that the convergence difficulties illustrated in Figs. 3 and 4 can be remedied by using an integral formulation of the scattering problem which is well behaved in all cases. There are several methods available for obtaining such a formulation. The method we consider in this paper is a combined field integral equation (CFIE) formulation of the

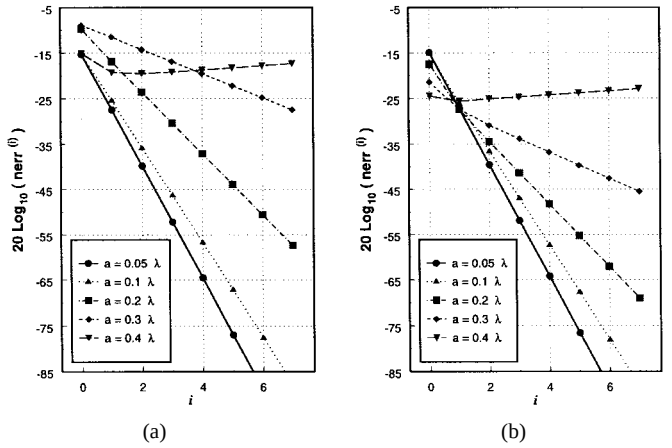

Fig. 3. Normalized residual error $\mathtt{nerr}^{(i)}$ versus iteration number for different radii and TM incidence using the (a) SIP and (b) SIX orderings. In both cases $\chi = 90^\circ$, $a/b = 1$.

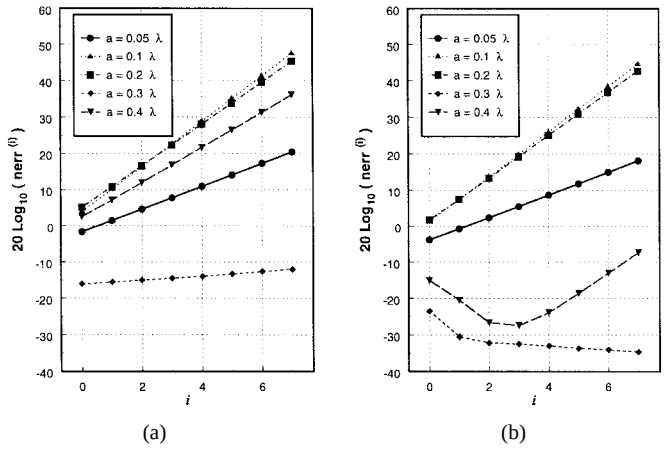

Fig. 4. Normalized residual error $\mathtt{nerr}^{(i)}$ versus iteration number for different radii and TE incidence using the (a) SIP and (b) SIX orderings. In both cases $\chi = 90^\circ$, $a/b = 1$.

scattering problem. The CFIE is a superposition of the MFIE and the electric field integral equation (EFIE)

$$\mathrm{CFIE}_\alpha \equiv \alpha\mathrm{EFIE} + \mathrm{MFIE} \tag{2}$$

where α is here taken to be a complex constant.

The use of MOMI with a CFIE formulation of the scattering problem introduces additional challenges. As previously noted, MOMI was originally developed for use with the MFIE. The kernel of the CFIE is a linear combination of the MFIE and EFIE kernels. In contrast to the nonsingular kernel of the TM and TE MFIE's, the EFIE kernels are singular. This singular behavior produces a coupling between sources on the surface of a scatterer which cannot be accommodated via the decoupled multiple scattering representation used by MOMI. This coupling is especially strong in the TM EFIE due to the presence of a hypersingular kernel and requires that a modified form of MOMI be used [12]–[14]. For this reason, in this paper, we restrict our consideration to the TE problem.

The parameter α appearing in the CFIE (2) is only minimally constrained in that it must have a nonzero imaginary component for the CFIE to provide a unique solution to the

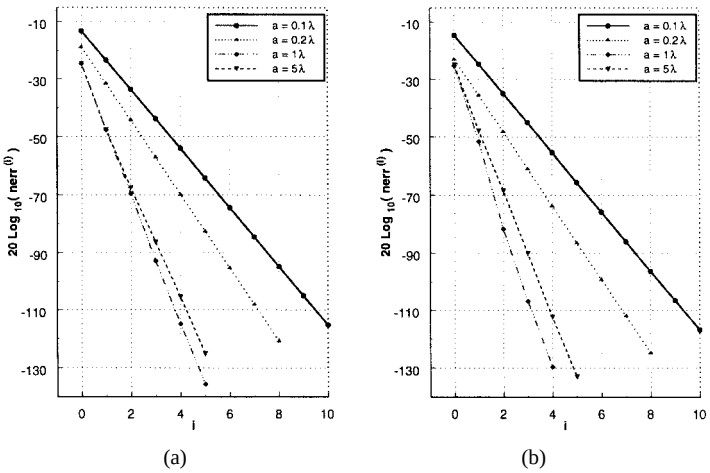

Fig. 5. Convergence of SIP and SIX MOMI series for TE scattering from circular cylinders of various radii $(\alpha = j\pi/\lambda, \chi = 90^\circ)$.

scattering problem.[1] We further constrain the choice of α by seeking the value of this parameter which minimizes the maximum eigenvalue of the propagator (i.e., the kernel of the MOMI integral equation, see below) in the MOMI reformulation of the resultant CFIE. This constraint produces an optimal iterative series in that the minimum rate of convergence is maximized for an arbitrary excitation. Asymptotic estimates of the optimal value of α are derived in the limits of large and small cylinders by minimizing the contribution of the integral term (i.e., the scattered field) appearing in the CFIE. Numerical computations demonstrate that the resultant closed-form estimates of the optimal CFIE are accurate. From these estimates we observe that the optimal CFIE formulation of the problem is a strong function of the size of the scatterer for small cylinders. For cylinders whose maximum dimension is on the order of one wavelength or larger, the optimal CFIE formulation is independent of the scatterer's size.

The convergence properties of the MOMI series obtained using the CFIE formulation, which is optimal in the limit of a large scatterer, are illustrated in Figs. 5 and 6. Fig. 5 considers scattering from circular cylinders $(a/b = 1)$ and Fig. 6 presents results for scattering from elliptical cylinders having $a/b = 8$. Table I shows the number of MOMI iterations needed to achieve a normalized residual error (defined below) of 10^{-3} for circular and elliptical cylinders. The required number of iterations is seen to be independent of the size of the scatterer over a three-orders-of-magnitude change in the circumference of the cylinder. The large number of required iterations observed for small cylinders is due to the use of a CFIE formulation which is optimal for large scatterers.

III. MOMI Iteration of Second-Kind Integral Equations

In the case of TM incidence on a sufficiently smooth surface, the second-kind integral equation satisfied by the y-directed

[1] In response to a reviewer comment, we note that the CFIE parameter α is often considered a real number. In our analysis α must satisfy $\mathrm{Im}(\alpha) \neq 0$ because of the form of the TE MFIE used in (4) below.

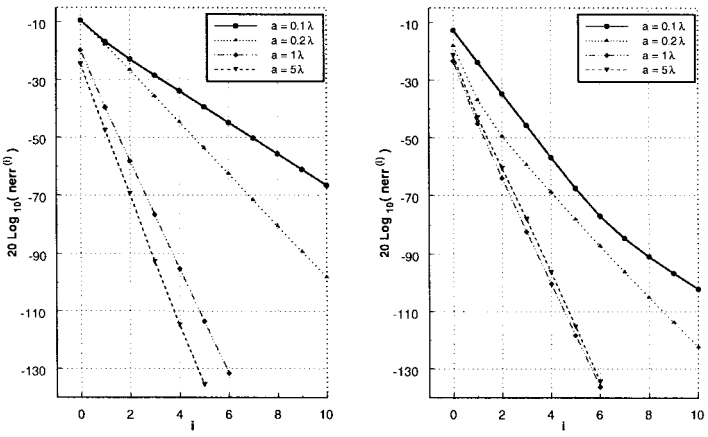

(a) (b)

Fig. 6. Convergence of SIP and SIX MOMI series for TE scattering from elliptical cylinders having an axial ratio $a/b = 8$ with various values of semi-major axis a ($\alpha = j\pi/\lambda, \chi = 90°$).

TABLE I
NUMBER OF MOMI ITERATIONS REQUIRED TO ACHIEVE $\mathtt{nerr}^{(i)} < 10^{-3}$. THE AVERAGE CONVERGENCE RATE FOR $a/b = 1$ WHEN $a > 0.5\lambda$ IS 22 (SIP) AND 22 (SIX) dB/ITERATION. FOR $a/b = 8$ THE AVERAGE RATES ARE 19 (SIP) AND 21 (SIX) dB/ITERATION

Major	$a/b = 1$		$a/b = 8$	
Axis	SIP	SIX	SIP	SIX
0.02 λ	27	27	77	91
0.1 λ	8	7	10	9
1 λ	2	2	3	2
2 λ	2	2	3	2
8 λ	2	2	3	2
32 λ	2	2	3	2
128 λ	2	2	3	2
512 λ	2	2	3	2
2048 λ	2	2	3	2

magnetic field is [7]

$$H = 2H^{\text{inc}} + 2\int_S H\frac{\partial G}{\partial n_o}\,dS_o \tag{3}$$

while in the case of TE incidence the normal derivative of the y directed E-field satisfies the second kind integral equation

$$\frac{\partial E}{\partial n} = 2\frac{\partial E^{\text{inc}}}{\partial n} - 2\int_S \frac{\partial E}{\partial n_o}\frac{\partial G}{\partial n}\,dS_o. \tag{4}$$

In both (3) and (4), G is the 2-D free-space Green's function

$$G(k_o|\boldsymbol{\rho} - \boldsymbol{\rho}_o|) = \frac{1}{j4}H_0^{(2)}(k_o|\boldsymbol{\rho} - \boldsymbol{\rho}_o|) \tag{5}$$

where $k^2 = \omega^2\mu\varepsilon$ and $H_0^{(2)}$ is the zeroth order Hankel function of the second kind and all quantities are to be evaluated on the surface of the cylinder. The unit-normal vector $\hat{\mathbf{n}}$ points out from the center of the ellipse.

The self-term contributions due to the first normal derivatives of the Green's function in (3) and (4) have been removed from the integral terms using an appropriate limiting procedure [9]. As a result, the kernel functions can be defined to be continuous [15]. Finally, in the case of a circular cylinder, the normal derivatives of the Green's function in (3) and (4) are given by

$$\frac{\partial G}{\partial n_o} = \frac{\partial G}{\partial n} = -\frac{k}{j4}\left|\sin\frac{\phi - \phi_o}{2}\right| H_1^{(2)}(k|\boldsymbol{\rho} - \boldsymbol{\rho}_o|) \tag{6}$$

where $H_1^{(2)}$ is the first-order Hankel function of the second kind.

A. Discretization of (3) and (4)

Equations (3) and (4) can be rewritten in operator form as

$$\Phi = \Phi^{\text{inc}} + \mathcal{P}\Phi \tag{7}$$

where

$$\mathcal{P}\Phi = \int_S K_0(\boldsymbol{\rho}, \boldsymbol{\rho}_o)\Phi(\boldsymbol{\rho}_o)\,dS_o \tag{8}$$

and $K_0(\boldsymbol{\rho}, \boldsymbol{\rho}_o)$ is termed either the propagator or kernel of the integral equation. The appropriate definitions of Φ, Φ^{inc}, and $K_0(\boldsymbol{\rho}, \boldsymbol{\rho}_o)$ are clear through a comparison of (8) with (3) and (4). We approximate the solution to (7) using pulse expansion and delta testing functions to discretize the integral equation (7) into a matrix equation of the form

$$\psi = \psi^{\text{inc}} + P\psi. \tag{9}$$

The details of the discretization procedure are provided in the Appendix.

B. Ordered Multiple Interactions Formulations of (9)

In developing MOMI to analyze scattering from extended rough surfaces, the self interaction terms P_{ii} were neglected [7]. The propagator matrix was thus decomposed into lower triangular (L) and upper triangular (U) matrices, each having zero entries along the diagonal

$$P \to L + U. \tag{10}$$

After a few simple manipulations, this decomposition led to the MOMI matrix equation (cf. [7, eq. (11)])

$$\psi = (I - U)^{-1}(I - L)^{-1}\psi^{\text{inc}} + (I - U)^{-1}(I - L)^{-1}LU\psi. \tag{11}$$

However, consistent discretization of (7) requires that the diagonal elements P_{ii} be retained. This modification can be incorporated into (11) in several ways. In applying MOMI to integral equations having singular kernels, it has been found that optimal convergence properties are obtained by decomposing the propagator matrix as

$$P = L + \hat{D} + U \tag{12}$$

where $\hat{D}$ is a diagonal matrix with $\hat{D}_{ii} = P_{ii}$. Physically, maintaining the self interaction terms in $\hat{D}$ separate from L and U provides better convergence properties when applying the method to integral equations having singular kernels because these equations exhibit strong coupling between oppositely directed fields on the surface of a scatterer [12].

Following a procedure analogous to that discussed in [7], the decomposition (12) leads to the matrix equation

$$\psi = (D-U)^{-1}D(D-L)^{-1}\psi^{\text{inc}} + P_M\psi \tag{13}$$

where $D = I - \hat{D}$ and the MOMI propagator P_M is defined as

$$P_M \equiv (D-U)^{-1}D(D-L)^{-1}LD^{-1}U. \tag{14}$$

Iteration of (13) yields the candidate solution

$$\psi = \sum_{n=0}^{\infty} P_M^n (D-U)^{-1}D(D-L)^{-1}\psi^{\text{inc}} \tag{15}$$

which is the same as [7, eq. (28)] under the substitution $D \to I$. Since $D = I + \mathcal{O}(\Delta x)$, the convergence properties of (15) are essentially unchanged from those of [7, eq. (28)]. When convergence occurs, the candidate solution (15) converges to the exact solution of (9). As discussed below, even in cases for which the infinite series does not converge, the first few terms of (15) can still provide a good approximation to the actual solution.

The MOMI series (15) provides a very robust and rapidly convergent solution to the MFIE for scattering from extended rough surfaces in two dimensions. These desirable properties have been attributed to the manner in which the MOMI series resums the multiple scattering terms present in the Neumann series for the original integral equation (7). The Born term in the MOMI series $(D-U)^{-1}D(D-L)^{-1}\psi^{\text{inc}}$ includes the contributions to the current due to all orders of continuous forward scattering ($(D-L)^{-1}$), all orders of backscattering ($(D-U)^{-1}$), and one order of interaction between the backward and forward traveling waves on the surface (resulting from the multiplication of these operators).

For this reason, the ordering of the unknowns in the original matrix equation (9) can have a drastic effect on the convergence of the MOMI series. This is in contrast to the Neumann series for (9) whose convergence properties are independent of the manner in which the unknowns are ordered in the matrix equation. A different ordering of unknowns in the MOMI series will result in the summation of different multiple scattering terms. In the case of a random ordering of the unknowns in the original matrix equation (9) for the rough surface scattering problem, the number of MOMI iterations required to converge to a given error tolerance can be significantly larger than in the case of the physically based forward/backward ordering.

It is not immediately clear how the unknowns in (9) should be ordered for the application of MOMI to closed-body scattering problems. In the case of elliptical cylinders, at least two ordering schemes incorporate important physical aspects of the scattering problem. These methods of ordering the unknowns in the matrix equation are illustrated in Fig. 2. An ordering which is sequential-in-ϕ (SIP) produces an iterative series which mimics the progression of creeping waves around the surface of the cylinder. An alternative approach is one which is sequential-in-x (SIX). This ordering results in a MOMI series for the closed-body problem, which is somewhat analogous to the forward/backward approach used in [7].

For either an SIP or SIX ordering of the unknowns, the MOMI series can still be written as indicated in (15). A reordering of the unknowns simply requires a corresponding redefinition of the matrices L, D, and U. For this reason, in the case of scattering from closed bodies, it is appropriate to speak of L and U as multiple scattering operators instead of the more specific forward and backward propagator designations used in the case of scattering from one-dimensional rough surfaces [16].

C. Solution of (9) Using (15) for TM and TE Scattering from Circular Cylinders

To facilitate the investigation of the properties of the proposed iterative solution (15) to the MOMI matrix equation (13), it is convenient to define the normalized residual error

$$\texttt{nerr}^{(i)} \equiv \frac{\left\| \{(D-U)^{-1}D(I-L)^{-1}LD^{-1}U\}^{i+1}\phi^{(0)} \right\|_2}{\left\| \phi^{(0)} \right\|_2}, \quad \text{for } i \geq 0 \tag{16}$$

where $\phi^{(0)}$ is the order zero iterate of the MOMI series. $\texttt{nerr}^{(i)}$ provides a measure of the error in the ith order iterative approximation $\psi^{(i)}$ obtained by truncated the infinite series (15) to $i+1$ terms.

Figs. 3 and 4 utilize this error norm to illustrate the convergence rates of the MOMI series for various radii in the cases of TM and TE incidence using SIP and SIX orderings of the surface current unknowns. From these examples it is apparent that the MOMI series for the MFIE is not nearly as robust as observed for the case of scattering from rough surfaces. In several cases, the series actually appears to be diverging. This is somewhat surprising given the physical interpretation of MOMI as a procedure for resumming the multiple scattering terms present in the Neumann series for the original integral equation.

Before further examining the cause of these convergence difficulties, it is instructive to consider the Born term of the MOMI series, i.e. the $n = 0$ term in (15). As is well known, the solution of the integral equation (7) is nonunique at a discrete set of radii corresponding to the zero-source solutions of the interior problem [9]. Figs. 7 and 8 illustrate the behavior of the Born term of the MOMI series at a resonant point of the interior problem. Also shown in these figures is the exact solution to the scattering problem obtained using a special function expansion technique [17]. For a proper choice of origin and proper ordering of the surface current unknowns, the Born term is seen to provide a good approximation to the actual solution. This implies that the MOMI series is able to incorporate the physically important multiple scattering interactions. Similar results are obtained away from resonance.

Fig. 9 shows the three largest eigenvalues of the MOMI propagator matrix P_M for TM scattering from circular cylinders with radii in the range 0 to 1.5λ. Fig. 10 shows similar results for the TE scattering problem. Although not indicated, the variation of these largest eigenvalues has been computed for cylinders having radii of up to 30λ and the same general pattern continues. There is no radius in the TE problem for which the largest modulus eigenvalue of P_M is less than one

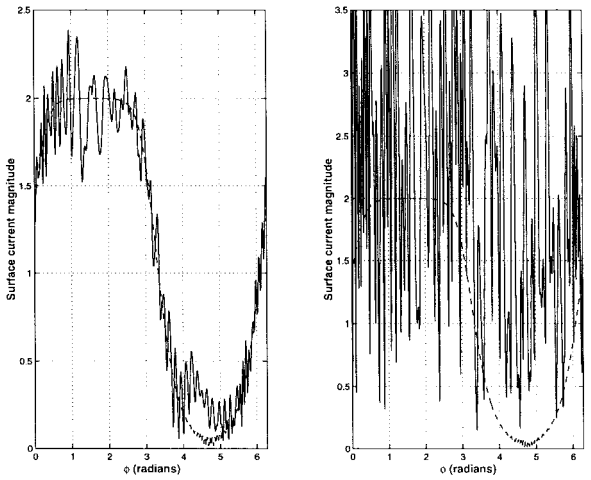

(a) (b)

Fig. 7. Born term of MOMI series obtained for TM scattering from a circular cylinder $(a = 7.375\,43\lambda)$ using an SIP ordering with (a) $\chi = 90^\circ$ and (b) $\chi = 180^\circ$. The dashed line is the exact solution.

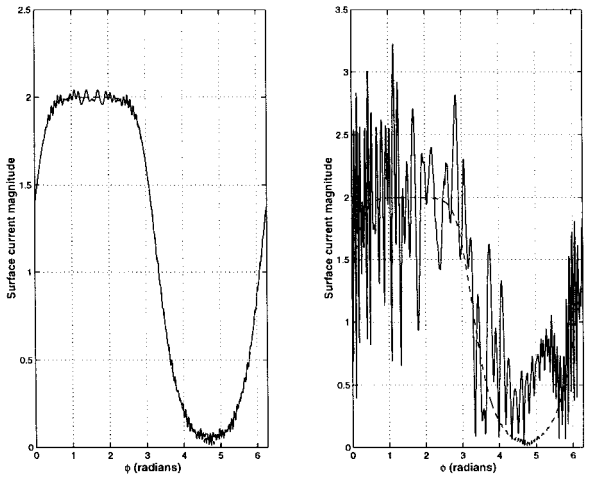

(a) (b)

Fig. 8. Born term of MOMI series obtained for TM scattering from a circular cylinder $(a = 7.375\,43\lambda)$ using an SIX ordering with (a) $\chi = 90^\circ$ and (b) $\chi = 180^\circ$. The dashed line is the exact solution.

and there is no radius above $a \approx 0.386\lambda$ in the TM problem (the first interior resonance point) for which the maximum eigenvalue modulus is less than unity.

The behavior of the eigenvalues of P_M illustrated in Figs. 9 and 10 explains the convergence properties of the MOMI series illustrated in Figs. 3 and 4. As illustrated in Fig. 9, for $a < 0.386\lambda$ the largest eigenvalue in the TM problem is less than unity and the MOMI series converges with the rate of convergence decreasing as the radius approaches this upper limit. For larger radii the series does not converge. In the TE problem convergence is not obtained even in the limit $a \to 0$ since the modulus of the largest eigenvalue is greater than or equal to unity for all values of the cylinder radius a (see Fig. 10). The differences between the SIP and SIX orderings in Figs. 3 through 8 result because the corresponding MOMI series incorporate different multiple scattering terms. Observe, however, that although the behavior of the SIP and SIX series

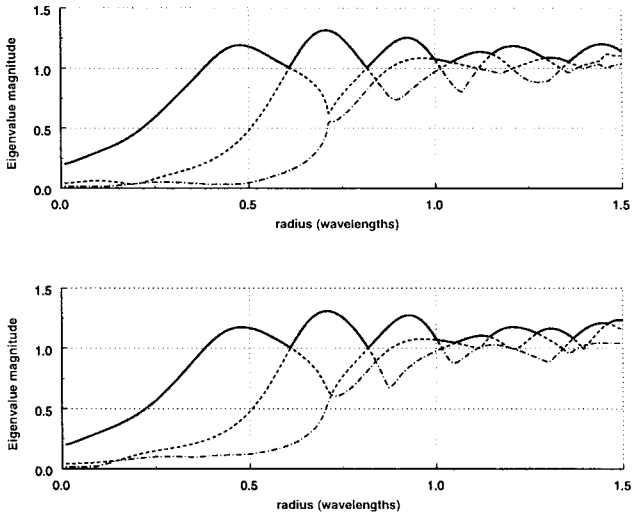

Fig. 9. Magnitude of three largest eigenvalues of P_M versus radius for the TM problem $(a/b = 1)$.

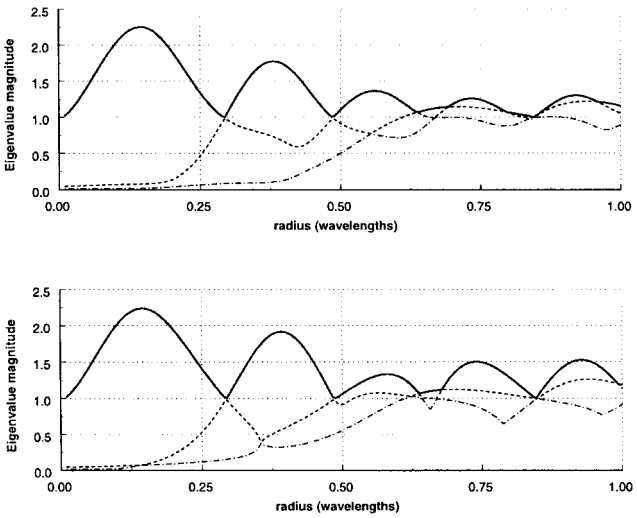

Fig. 10. Magnitude of three largest eigenvalues of P_M versus radius for the TE problem $(a/b = 1)$.

in Figs. 3 through 8 are significantly different, the behavior of the three largest modulus eigenvalues is very similar. This suggests that the convergence difficulties of MOMI when applied to the MFIE are largely independent of the ordering scheme chosen.

D. Interpretation

The general failure of the MOMI series as applied to the MFIE for scattering from circular cylinders is somewhat surprising given the interpretation of MOMI as a method for resumming the multiple scattering terms in the Neumann series for the original matrix equation [7]. To better understand this failure we observe that the MOMI propagator can be rewritten as

$$\begin{aligned} P_M &= (I-U)^{-1}(I-L)^{-1}LU \\ &= (I-U)^{-1}(I-L)^{-1}[(I-L)(I-U)-(I-P)] \\ &= I-(I-U)^{-1}(I-L)^{-1}(I-P) \end{aligned} \tag{17}$$

where for simplicity we have replaced $D \to I$ and $P = L+U$.

Thus, for (15) to exhibit desirable convergence properties we must have

$$(I-U)^{-1}(I-L)^{-1}(I-P)\approx I. \tag{18}$$

For this approximation to be good the decoupled inverse $(I-U)^{-1}(I-L)^{-1}$ must closely approximate the inverse of $(I-P)$. At and near resonance, however, $(I-P)$ is singular or nearly singular. In contrast, $(I-L)$ and $(I-U)$ are always well-behaved as they correspond to Volterra integral equations of the second kind having nonsingular kernels [18]. Thus, we should not expect MOMI to provide good convergence properties when applied to the MFIE formulation of the closed-body problem.

This convergence failure is equivalently understood by observing that in attributing the convergence success of the MOMI series to its ability to resum the terms in the Neumann series for the original matrix equation, it is implicitly assumed that coupling between the L and U components of the original matrix equation is weak and can be accommodated via decoupled forward and backward iterations. This assumption makes good physical sense in the PEC rough surface problem to which MOMI was originally applied. However, the MFIE formulation of the closed body scattering problem gives rise to a much stronger coupling between surface currents which cannot be recovered via the MOMI decoupled multiple scattering approximation.

IV. A Combined Field Formulation

Given this understanding, we next consider a formulation of the scattering problem which does not give rise to a singular or nearly singular integral equation. Several such methods are available (e.g., [19]–[22]). In the following, we consider a CFIE representation [22]. The CFIE is a linear combination of the MFIE and the EFIE as indicated above in (2).

While the CFIE can be used to provide a unique solution to the scattering problem, the use of MOMI as formulated in (15) with a combined field description of the scattering problem introduces additional difficulties associated with the kernels of the EFIE's. The EFIE kernel for the TE problem is simply the Green's function (5) of the Helmholtz equation. For TM scattering, the kernel function is the second normal derivative of the Green's function [9]. In applying the MOMI series to scattering from dielectric surfaces, it has been found that the singularities of these kernel functions produce strong coupling between oppositely directed fields [12]. The singularity present in the EFIE for TM scattering is particularly strong and requires that a modified form of (15) be used. The singularity of the EFIE kernel for TE scattering is much weaker and is, therefore, more amenable to the MOMI series solution technique. For this reason, in the following we investigate the application of MOMI to the CFIE for TE scattering only.

A. Selecting an Optimal CFIE: A Multiple Scattering Approach

The EFIE for TE scattering from a PEC object is [9]

$$0=E^{\text{inc}}-\int_S \frac{\partial E}{\partial n_o}G\,dS_o. \tag{19}$$

The CFIE for the TE case is obtained by adding this to the MFIE for this problem (4) using the complex constant α. This leads to

$$\frac{\partial E}{\partial n}=2\alpha E^{\text{inc}}+2\frac{\partial E^{\text{inc}}}{\partial n}-2\int_S \frac{\partial E}{\partial n_o}K_\alpha\,dS_o \tag{20}$$

where

$$K_\alpha\equiv\left(\alpha G+\frac{\partial G}{\partial n}\right). \tag{21}$$

Discretization of this equation is discussed in the Appendix. The resulting matrix equation can be put in the form of (9). The corresponding MOMI series is of the same form as (15).

The CFIE (20) is guaranteed to have a unique solution whenever α has a nonzero imaginary component [22]. This requirement provides significant freedom in the choice of α. We further constrain α by requiring that it provide optimal convergence properties for an arbitrary incident field. This corresponds to the value of α which minimizes the maximum modulus eigenvalue of P_M.

A physically intuitive way of determining this optimal choice is to minimize the contributions to the total field in (20), which are due to the integral term. Observe that if α is chosen such that $K_\alpha\equiv 0$ then no iteration is required to obtain the exact solution to the scattering problem. This is physically interpreted as the case of zero multiple scattering, an example of which occurs in the MFIE $(\alpha=0)$ formulation of scattering from an infinite PEC planar surface. In this case

$$\frac{\partial G}{\partial n}\equiv 0 \tag{22}$$

and the integral term in (20) provides no contribution to the total surface current. This results for the flat surface scattering problem because the magnetic field radiated to an observation point on the surface by sources that are also on the surface has no tangential component. Thus, the MFIE for which MOMI was originally developed can be viewed as the specialization of (20) to the rough surface case where α is selected such that K_α is identically zero in the unperturbed geometry of the rough surface scattering problem.

If possible, the optimal choice for α would in general be

$$\alpha=-\frac{1}{G}\frac{\partial G}{\partial n} \tag{23}$$

as this would give $K_\alpha\equiv 0$ in all cases. Because this choice is not generally possible, we instead consider asymptotically determined estimates of α. In addition to providing optimal integral formulations, these asymptotic estimates provide information on how the optimal value of α depends on the size and shape of the scatterer. To simplify the following analysis, we consider only the case of circular cylinders for which the normal derivative of the Green's function is given in (6).

For small cylinder radii $(ka\ll 1)$, the normal derivative of the electric field on the surface is approximately constant. Thus

$$\int_S \frac{\partial E}{\partial n}K_\alpha\,dS_o\approx\frac{\partial E}{\partial n}\int_S K_\alpha\,dS_o \tag{24}$$

and the contribution of the integral term to the total field in (20) is minimized by choosing

$$\alpha = -\frac{\langle \partial G/\partial n \rangle}{\langle G \rangle} \tag{25}$$

where $\langle \cdot \rangle$ denotes an average of the source point over the surface of the cylinder. Using the small argument forms of the zero and first order Hankel functions [23]

$$\begin{aligned} H_0^{(2)}(z) &\sim 1 - \frac{j2}{\pi}\left[\ln\left(\frac{z}{2}\right) + \gamma\right] \\ H_1^{(2)}(z) &\sim \frac{j2}{\pi z} \end{aligned} \tag{26}$$

in (25) gives

$$\begin{aligned} \alpha &\sim \frac{j2}{a}\left\langle \left(1 - \frac{j2\gamma}{\pi}\right) - \frac{j2}{\pi}\ln\left(ka\left|\sin\frac{\phi-\phi_o}{2}\right|\right)\right\rangle^{-1} \\ &= -\frac{1}{a}[j\pi + 2(\ln(ka) - \ln 2 + \gamma)]^{-1} \end{aligned} \tag{27}$$

which is seen to be inversely related to the size of the cylinder.

For large cylinder radii ($ka \gg 1$) the approximation (24) is not valid. Instead we attempt to minimize the contribution of the integral term appearing in (20) by choosing for α the average of (23), i.e.,

$$\alpha = -\left\langle \frac{\partial G/\partial n}{G} \right\rangle. \tag{28}$$

Substituting the large argument forms of the zero and first-order Hankel functions [23]

$$\begin{aligned} H_0^{(2)}(z) &\sim \sqrt{\frac{2}{\pi z}} e^{-j(z-\pi/4)} \\ H_1^{(2)}(z) &\sim \sqrt{\frac{2}{\pi z}} e^{-j(z-3\pi/4)} \end{aligned} \tag{29}$$

simplifies (28) to[2]

$$\alpha \sim jk\left\langle \left|\sin\frac{\phi-\phi_o}{2}\right| \right\rangle = \frac{j2k}{\pi} = \frac{j4}{\lambda}. \tag{30}$$

Unlike the small ka limit (27) for which the optimal choice of α was found to vary with a, the value of α suggested by (30) is independent of the cylinder's size.

The physical significance of the value of α given by (30) is understood by observing that, on the surface of the cylinder in the TE problem

$$\frac{\partial E}{\partial n}\hat{\mathbf{y}} = j\omega\mu\hat{\mathbf{n}} \times \mathbf{H} = j\omega\mu H_{\tan}\hat{\mathbf{y}}. \tag{31}$$

Multiplying this equation through by α^{-1} and inserting the asymptotic value of α given by (30) prior to averaging (i.e., $\alpha = jk|\sin(\phi-\phi_o)/2|$) we have

$$\begin{aligned} \frac{1}{\alpha}\frac{\partial E}{\partial n} &= \frac{j\omega\mu}{jk\left|\sin\frac{\phi-\phi_o}{2}\right|} H_{\tan} \\ &= \tilde{\eta} H_{\tan} \end{aligned} \tag{32}$$

[2] Although the averaging performed in (30) has been performed over all ϕ_o, the contributions to the average from points near the observation point (for which the large argument approximations of the Hankel functions are not valid) are negligible when ka is large.

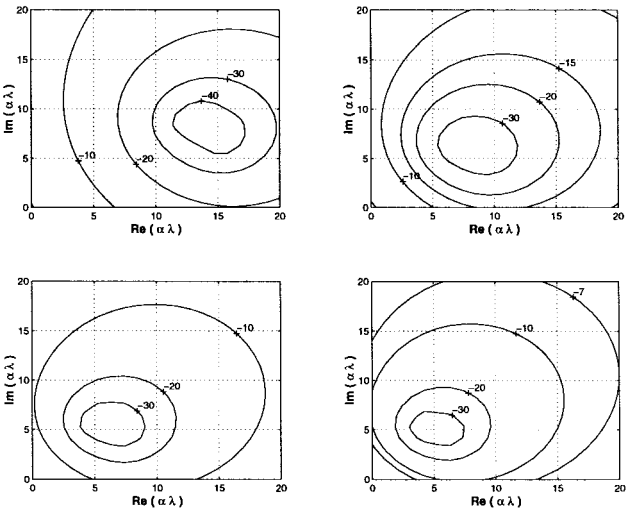

Fig. 11. Contours of largest eigenvalue in decibels of P_M as a function of the complex constant α for circular cylinders (SIP ordering).

where

$$\tilde{\eta} \equiv \frac{\eta}{\left|\sin\frac{\phi-\phi_o}{2}\right|} \tag{33}$$

and η is the free-space impedance $\eta = \sqrt{\mu/\varepsilon}$. Recalling that a plane wave propagating in the $\hat{\mathbf{k}}$ direction satisfies the relation

$$\eta\hat{\mathbf{k}} \times \mathbf{H} = -\mathbf{E} \tag{34}$$

we see that the choice of α specified by (30) results from the fact that the field at an observation point excited by a distant source point is locally planar. The $|\sin(\phi-\phi_o)/2|$ in the denominator of (33) [which is not present in (34)] arises because the CFIE imposes a boundary condition on the tangential components of the total field. For TE incidence, the electric field is always tangential to the cylinder while the component of the magnetic field tangent to the cylinder varies with the location of the source point.

The optimality of the asymptotic estimates for α provided by (27) and (30) can be evaluated by calculating the eigenvalues of the resulting propagator matrices P_M. Figs. 11 and 12 show the magnitude of the largest eigenvalue of the MOMI propagator P_M for the TE CFIE (20) as a function of the complex constant α for various cylinder radii. Table II contains the values of α predicted by (25), (27), and (30).

As anticipated by the above asymptotic analysis, for small radii, the choice of α, which yields the minimum maximum eigenvalue of P_M, varies significantly with the radius of the cylinder. The estimates of α provided by (25) and (27) are good through $a = 0.05\lambda$. Equation (25) provides a good estimate of the optimal value of α for $a = 0.2\lambda$. For the larger radii cases of $a = 1\lambda$ and $a = 5\lambda$, the value of α which yields the minimum maximum eigenvalue remains fairly constant at $\alpha \approx j4/\lambda$, which is in good agreement with the asymptotic value provided by (30).

From these figures we also notice that the minimum maximum eigenvalue of P_M as a function of α increases as the cylinder radius increases from 0.01λ to 5λ. This occurs because for large cylinder radii we are able to minimize the

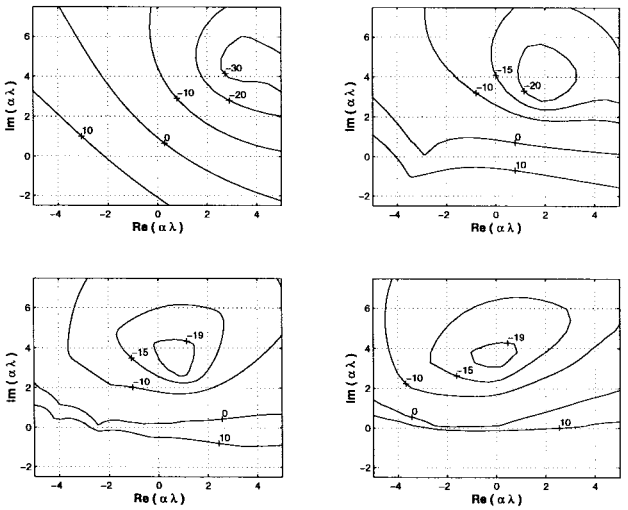

Fig. 12. Contours of largest eigenvalues in decibels of P_M as a function of the complex constant α for circular cylinders (SIP ordering).

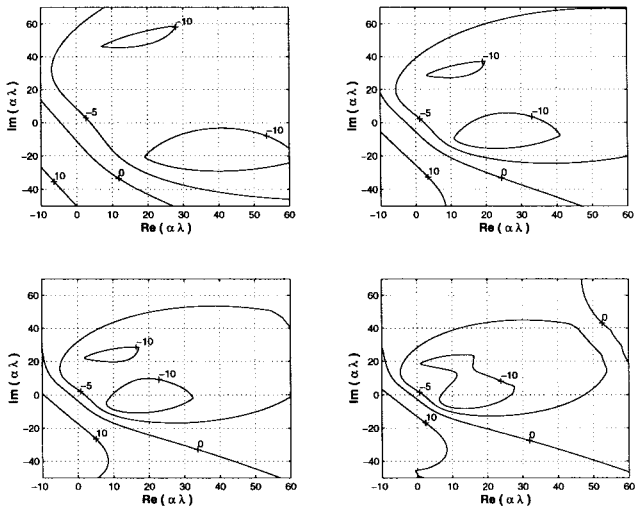

Fig. 13. Contours of largest eigenvalues in decibels of P_M as a function of the complex constant α for elliptical cylinders having $a/b = 8$ (SIP ordering).

TABLE II
ASYMPTOTIC ESTIMATES OF THE OPTIMAL CHOICES FOR α. ESTIMATES FROM BOTH EQUATIONS (25) AND (27) ARE PROVIDED TO DEMONSTRATE THAT THE ASYMPTOTIC FORM (27) PROVIDES INACCURATE RESULTS BEFORE THE ESTIMATE (25) BREAKS DOWN (cf. $a = 0.2\lambda$ CASE)

Cylinder Radius	$\alpha\lambda$ from Eqn (25)	$\alpha\lambda$ from Eqn (27)	$\alpha\lambda$ from Eqn (30)
0.01 λ	$13.60 + j7.30$	$13.37 + j7.28$	$j4$
0.02 λ	$8.00 + j5.46$	$7.54 + j5.41$	$j4$
0.03 λ	$5.95 + j4.74$	$5.26 + j4.63$	$j4$
0.04 λ	$4.90 + j4.35$	$3.97 + j4.17$	$j4$
0.05 λ	$4.26 + j4.10$	$3.11 + j3.84$	$j4$
0.2 λ	$3.66 + j3.31$	$-0.11 + j1.58$	$j4$
1 λ	$-2.78 + j3.15$	$-0.16 + j0.14$	$j4$
5 λ	$-3.06 + j3.14$	$-0.02 + j0.01$	$j4$

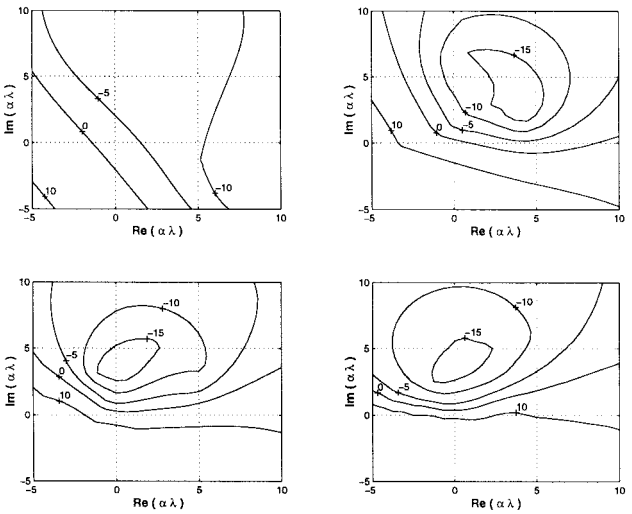

Fig. 14. Contours of largest eigenvalues in decibels of P_M as a function of the complex constant α for elliptical cylinders having $a/b = 8$ (SIP ordering).

integral term's contribution to (20) only by minimizing K_α in an average sense. In the small radius limit the approximation in (24) allowed us to determine the value of α by minimizing the contribution from the integral term itself.

Figs. 13 and 14 show the magnitude of the largest eigenvalue of P_M for TE scattering from elliptical cylinders having axial ratios of $a/b = 8$. For small radii we see that the optimal choice of α changes significantly with the size of the ellipse. The smallest maximum eigenvalue of P_M is larger for small elliptical cylinders than for small circular cylinders due to the breakdown of approximation (24) as the axial ratio a/b increases. Also note that the optimal choice of α appears to bifurcate into two distinct regions in the complex α-plane for small a. This is due to the loss of rotational symmetry when $a/b \neq 1$ and suggests that it may be more appropriate to choose α as a function of position in this case, i.e., $\alpha = \alpha(\boldsymbol{\rho})$. For larger values of a the estimate in (30) derived for circular cylinders is seen to provide an excellent choice in the case of $a/b = 8$.

B. Effect of Asymptotically Optimal α on Eigenvalues of P

The preceding determination of the asymptotically optimal choices for α was motivated by the physical consideration that the eigenvalues of P_M are related to the multiple scattering contribution of the integral term appearing in (20) to the total surface current. Since the optimal choice of α was determined without reference to the MOMI reformulation of the problem, it is informative to consider the effect of this choice on the eigenvalues of the propagator P of the original integral equation. The eigenvalues of the propagator P associated with (20) are [24]

$$\xi_m = 1 - \frac{2J_m'(ka) + \frac{2\alpha}{k}J_m(ka)}{J_m'(ka) + \eta_m^{\mathrm{TE}} H_m^{(2)'}(ka)} \tag{35}$$

where

$$\eta_m^{\mathrm{TE}} = -\frac{J_m(ka)}{H_m^{(2)}(ka)}. \tag{36}$$

In the small radius limit for $m = 0$ (35) reduces to

$$\xi_0 \sim 1 - 2\alpha a\left(\frac{\pi}{j2} - \gamma - \ln\frac{ka}{2}\right) \tag{37}$$

where $\gamma \approx 0.577$ is Euler's gamma. When $m \neq 0$ (35) becomes

$$\xi_m \sim -\alpha\frac{a}{m} \tag{38}$$

where m must be sufficiently small relative to ka for this to provide a good approximation. This limitation arises because the asymptotic expressions used to derive this result from (35) are not uniformly valid with respect to m.

Inserting the asymptotic value of α given by (27) into (37) and (38) we have that $\xi_0 \sim 0$ while

$$\xi_m \sim \frac{1}{m}[j\pi + 2(\ln(ka) - \ln 2 + \gamma)]^{-1} \quad \text{for } |m| = 1, 2, 3, \cdots. \tag{39}$$

Thus, the asymptotic value of α given in (27) is the value for which $\xi_0 \sim 0$ as $ka \to 0$. This is not surprising since the eigenfunction associated with ξ_0 is a constant. This corresponds to the constant surface current assumption made in (24) in determining the optimal value of α in the small radius limit. The m^{-1} decay of the ξ_m specified by (39) is likely the result of integrating the relatively slowly varying kernel K_α in the small radius limit against the surface current eigenfunctions $e^{jm\phi}$.

In the limit of large ka (35) reduces to

$$\xi_m \sim \frac{\sin(\beta) + \left(j - \frac{2\alpha}{k}\right)\cos(\beta)}{-\sin(\beta) + j\cos(\beta)} \tag{40}$$

where $\beta \equiv ka - \frac{m\pi}{2} - \frac{\pi}{4}$. As above, this asymptotic form of ξ_m is valid only for m sufficiently small such that the asymptotic forms of the Bessel functions used to derive this result are valid. In this limit, the modulus of ξ_m is minimized over all β for each m when $\alpha = jk/2 = j\pi/\lambda$. This result is close to the value of $j4/\lambda$ specified in (30). Thus, in both the large and small ka limits, the asymptotically optimal estimates of α derived above also minimize the maximum modulus of a class of eigenvalues of the propagator P.

C. Convergence of the MOMI Series for Scattering from Elliptical Cylinders

The asymptotically optimal values of α have been determined by requiring that they minimize the maximum eigenvalue of P_M as this provides an upper bound on the number of MOMI iterations required to achieve a given error tolerance for an arbitrary excitation. We now consider the convergence of the resultant series for the physically realistic case of an incident plane wave. Furthermore, since we are typically interested in achieving a rapid rate of convergence for large scatterers, in the following, we choose $\alpha = j\pi/\lambda$ in all cases.

The convergence of the MOMI series for the TE CFIE (20) for this choice of α is illustrated in Figs. 5 and 6 for SIP and SIX unknown orderings for scattering from elliptical cylinders having axial ratios of $a/b = 1$ (Fig. 5) and $a/b = 8$ (Fig. 6) and various values of the semimajor axis length a. From these figures it is apparent that both SIP and SIX orderings of the surface current unknowns produce rapidly convergent series for medium to large-sized cylinders. The slower rate observed for the small cylinders results because of the value of α used. To obtain a rapid convergence rate in these cases α should be chosen according to (27).

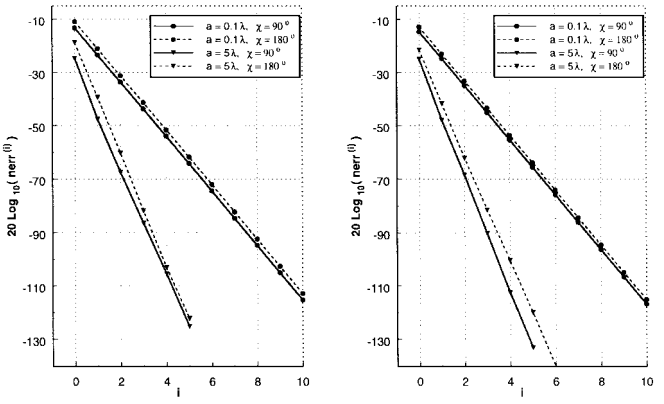

Fig. 15. Dependence of convergence rates of SIP and SIX MOMI series on choice of unknown origin for TE plane wave scattering from circular cylinders having radii values of $a = 0.1\lambda$ and $a = 5\lambda$ ($\alpha = j\pi/\lambda$).

In Fig. 15 we consider the effect of the choice of unknown origin on the convergence properties of the MOMI series. Previously, it was demonstrated that the accuracy of the Born term of the MOMI series for the MFIE depends strongly on the choice of unknown origin (cf. Figs. 7 and 8). The present figure demonstrates that for the examples chosen the convergence rate of the MOMI series for the CFIE is relatively insensitive to the choice of unknown origin.

Finally, in Table I the number of MOMI iterations required to achieve a normalized residual error less than 10^{-3} is given as a function of the semi-major axis a for an incident TE plane wave and $\alpha = j\pi/\lambda$. The number of required iterations appears to reach an asymptotically constant value of two or three for the examples chosen. It should be noted that, since the calculation of the Born term of the MOMI series requires the same computational effort as the other terms in the series, the computational effort required to obtain the second iterate of the MOMI series is similar to that required to compute the third iterate in the Neumann series for the original matrix equation (9).

V. Conclusion

The MOMI series exhibits poor convergence properties when used with the MFIE formulation of the closed-body scattering problem. This result is somewhat surprising given the physical interpretation of the MOMI series presented in [7] for extended rough surfaces. We have suggested that these poor convergence properties are due to the use of an integral representation which contains internal resonance points. A properly chosen combined field formulation of the TE problem has been shown to ameliorate these difficulties.

A method of determining the asymptotically optimal CFIE has been proposed using a multiple scattering interpretation of the integral term appearing in this equation. It has been demonstrated that the resultant estimate of the optimal CFIE

corresponds also to the minimization of a class of eigenvalues of the CFIE's propagator matrix. For small elliptical cylinders, the optimal integral formulation has been shown to depend strongly on the cross sectional size of the cylinder. However, for elliptical cylinders having major axis lengths on the order of a wavelength or larger, the optimal integral formulation quickly approaches an asymptotically constant limit.

The resultant MOMI series in the large scatterer limit converges rapidly. The number of iterations required to achieve a normalized residual error of 10^{-3} was observed to be independent of the electromagnetic size of the scatterer for elliptical cylinders having major axis lengths in the range of 1–2048 wavelengths and axial ratios of one and eight. This is in contrast to conjugate gradient iteration of the CFIE for which the number of iterations increases with the size of the cylinder [25]. Furthermore, we note that MOMI can be viewed as a preconditioning procedure to which a Krylov iterative scheme can be applied. This was not necessary here due to the rapid convergence of (15).

We are currently investigating the extension of the approach presented in this paper to the TM problem. This requires an extension of the MOMI method to more adequately account for singular kernels. Two methods of achieving this generalization have been developed for extended rough surfaces [13], [14]. It is anticipated that these results will also lead to improved convergence properties for the MOMI series discussed here. An alternative method for handling singular kennels is discussed in [11]. Finally, we are also investigating the use of MOMI with other methods which provide resonance-free formulations of the closed body scattering problem, as well as the application of MOMI to more complicated scatterers. The use of MOMI with a dual-surface MFIE formulation [21] of a corner scatterer is discussed in [26].

APPENDIX

In this appendix, we consider the discretization of (3), (4), and (20). Since the discretization procedure used for (3) is the same as that used for (4) and since (4) is a special case of (20), we only consider the discretization of (20) here.

A moment-method procedure [3] with pulse basis and delta testing functions is used to translate the infinite-dimensional CFIE into a finite-dimensional matrix equation having the form

$$\psi = \psi^{\mathrm{inc}} + P\psi. \tag{41}$$

The central angle ϕ is sampled uniformly such that $\Delta\phi = 2\pi/N$ where N is the number of pulse-expansion functions used. We evaluate all resultant integrals over the expansion functions to order $\Delta\phi$. The vector ψ contains the N expansion coefficients. ψ^{inc} contains the pointwise samples of the forcing term in the CFIE evaluated at the center of the angular interval over which each pulse-basis function is defined. Thus, for an unknown ordering which is SIP having an unknown origin of χ (cf. Fig. 2), the entries of the vector ψ^{inc} are given by

$$\psi_i^{\mathrm{inc}} = 2\left(\alpha E^{\mathrm{inc}} + \frac{\partial E^{\mathrm{inc}}}{\partial n}\right)_{\phi=\phi_i} \tag{42}$$

where $\phi_i \equiv i\Delta\phi - \Delta\phi/2 + \chi$. Using this discretization procedure, the off-diagonal elements of the propagator matrix P are

$$P_{ij} = -2K_\alpha(\boldsymbol{\rho}_i, \boldsymbol{\rho}_j)\Delta S_j \quad i \neq j \tag{43}$$

where K_α is defined in (21) and, for an ellipse having semi-major and semi-minor axis lengths a and b

$$\begin{aligned} \Delta S_j &= \Delta\phi\left[\rho(\phi)\left(1+\left(\frac{1}{\rho}\frac{\partial\rho}{\partial\phi}\right)^2\right)^{1/2}\right]_{\phi=\phi_j} \\ \rho(\phi) &= a[1+(r^2-1)\sin^2\phi]^{-1/2} \\ \frac{1}{\rho}\frac{\partial\rho}{\partial\phi} &= -\frac{1}{2}\sin 2\phi[r^2-1][1+(r^2-1)\sin^2\phi]^{-1} \end{aligned} \tag{44}$$

where $r \equiv a/b$. To determine the diagonal elements of the propagator matrix we recognize that the MFIE kernel function is well defined as $\boldsymbol{\rho} \to \boldsymbol{\rho}_o$ [15]. The contribution to the diagonal term associated with the EFIE kernel in the TE case contains a logarithmic singularity which can be integrated. This leads to the following result for the diagonal elements of TE CFIE propagator:

$$\begin{aligned} P_{ii} = {} & \frac{\Delta\phi}{\pi}\frac{r^2}{1+r^4-(r^4-1)\cos 2\phi_i} \\ & + \alpha\frac{a\Delta\phi}{\pi}\frac{u_1}{u_2}\left[\gamma - 1 + j\frac{\pi}{2} + \ln\left(\frac{ka}{2}u_3\Delta\phi\right)\right] \end{aligned} \tag{45}$$

where

$$\begin{aligned} u_1 &= \left[1+\frac{(r^2-1)^2\sin^2 2\phi_i}{4(1+(r^2-1)\sin^2\phi_i)^2}\right]^{\frac{1}{2}} \\ u_2 &= [1+(r^2-1)\sin^2\phi_i]^{\frac{1}{2}} \\ u_3 &= \left[\frac{1+r^4-(r^4-1)\cos 2\phi_i}{(1+r^2-(r^2-1)\cos 2\phi_i)^3}\right]^{\frac{1}{2}} \end{aligned} \tag{46}$$

For all cases considered in this paper, we have chosen N such that

$$\frac{a}{N} \leq \frac{\lambda}{100}. \tag{47}$$

ACKNOWLEDGMENT

The views and conclusions contained herein are those of the authors and should not be interpreted as necessarily representing the official policies or endorsements, either expressed or implied, of the Air Force Office of Scientific Research or the U.S. Government.

REFERENCES

[1] E. K. Miller, "A selective survey of computational electromagnetics," *IEEE Trans. Antennas Propagat.*, vol. 36, pp. 1281–1305, Sept. 1988.
[2] W. C. Chew, J. H. Jin, C. C. Lu, E. Michielssen, and J. M. Song, "Fast solution methods in electromagnetics," *IEEE Trans. Antennas Propagat.*, vol. 45, no. 3, pp. 553–543, Mar. 1997.
[3] R. F. Harrington, *Field Computation by Moment Methods*. Piscataway, NJ: IEEE Press, 1993.
[4] A. F. Peterson and R. Mittra, "Convergence of the conjugate gradient method when applied to matrix equations representing electromagnetic scattering problems," *IEEE Trans. Antennas Propagat.*, vol. AP-34, pp. 1447–1454, Dec. 1986.

[5] C. F. Smith, A. F. Peterson, and R. Mittra, "The biconjugate gradient method for electromagnetic scattering," *IEEE Trans. Antennas Propagat.*, vol. 38, pp. 938–940, June 1990.
[6] R. J. Adams and G. S. Brown, "On the use of the fast multipole method with the method of ordered multiple interactions," *Electron. Lett.*, vol. 34, pp. 2219–2220, Nov. 1998.
[7] D. A. Kapp and G. S. Brown, "A new numerical method for rough-surface scattering calculations," *IEEE Trans. Antennas Propagat.*, vol. 44, pp. 711–721, May 1996.
[8] R. J. Adams, R. Awadallah, J. Toporkov, and G. S. Brown, "Computational methods for rough surface scattering: The method of ordered multiple interactions," in *Proc. 4th Int. SIAM Conf. Math. Numer. Aspects Wave Propagat.*, Golden, CO, June 1998, pp. 79–83.
[9] N. Morita, N. Kumagai, and J. R. Mautz, *Integral Equation Methods for Electromagnetics*. Norwood, MA: Artech House, 1990.
[10] J. M. Elson, P. Tran, and F. J. Escobar, "Application of the MOMI method to the magnetic field integral equation," in *Radar Processing, Technol., Applicat. Proc. SPIE Photon. West Conf.*, San Diego, CA, July 1997, pp. 29–37.
[11] D. Torrungrueng and E. H. Newman, "The multiple sweep method of moments (MSMM) analysis of electrically large bodies," *IEEE Trans. Antennas Propagat.*, vol. 45, pp. 1252–1258, Aug. 1997.
[12] R. J. Adams and G. S. Brown, "Scattering from randomly rough dielectric surfaces using the method of ordered multiple interactions," in *Proc. Int. Conf. Electromagn. Adv. Applicat.*, Torino, Italy, Sept. 1997, pp. 359–361.
[13] ——, "An iterative solution for two-dimensional rough surface scattering problems based on a factorization of the Helmholtz operator," *IEEE Trans. Antennas Propagat.*, to be published.
[14] ——, "An iterative procedure for two first kind integral equations of scattering theory," *Radio Sci.*, to be published.
[15] J. V. Toporkov, R. T. Mar.and, and G. S. Brown, "On the discretization of the integral equation describing scattering by rough conducting surfaces," *IEEE Trans. Antennas Propagat.*, vol. 46, pp. 150–161, Jan. 1998.
[16] D. Holliday, L. L. DeRaad Jr., and G. J. St-Cyr, "Forward-backward: A new method for computing low-grazing scattering," *IEEE Trans. Antennas Propagat.*, vol. 44, pp. 722–729, May 1996.
[17] R. F. Harrington, *Time-Harmonic Electromagnetic Fields*. New York: McGraw Hill, 1961.
[18] A. C. Pipkin, *A Course on Integral Equations*. Boston, MA: Springer-Verlag, 1991.
[19] N. Engheta, W. D. Murphy, V. Rokhlin, and M. S. Vassiliou, "The fast multipole method (FMM) for electromagnetic scattering problems," *IEEE Trans. Antennas Propagat.*, vol. 40, pp. 634–641, June 1992.
[20] W. D. Murphy, V. Rokhlin, and M. S. Vassiliou, "Acceleration methods for the iterative solution of electromagnetic scattering problems," *Radio Sci.*, vol. 28, no. 1, pp. 1–12, 1993.
[21] M. B. Woodworth and A. D. Yaghjian, "Derivation, application, and conjugate gradient solution of dual-surface integral equations for three-dimensional, multiwavelength perfect conductors," in *PIER 5: Application of Conjugate Gradient Method to Electromagnetics and Signal Analysis*, J. A. Kong and T. A. Sarkar, Eds. New York: Elsevier, 1991, ch. 4.
[22] J. R. Mautz and R. F. Harrington, "H-field, E-field, and combined-field solutions for conducting bodies of revolution," *Archiv Elektronik Uebertragungstechnik (Electron. Communicat.)*, vol. 32, no. 4, pp. 157–164, 1978.
[23] M. Abramowitz and I. E. Stegun,Eds., *Handbook of Mathematical Functions*. New York: Dover, 1980 (9th printing).
[24] A. F. Peterson, "The "interior resonance" problem associated with surface integral equations of electromagnetics: Numerical consequences and a survey of remedies," *Electromagn.*, vol. 10, pp. 293–312, 1990.
[25] D. R. Wilton and J. E. Wheeler III, "Comparison of convergence rates of the conjugate gradient method applied to various integral equation formulations," in *PIER 5: Application of Conjugate Gradient Method to Electromagnetics and Signal Analysis*, J. A. Kong and T. A. Sarkar, Eds. New York: Elsevier, 1991, ch. 5.
[26] R. J. Adams and G. S. Brown, "A rapidly convergent iterative method for two-dimensional closed body scattering problems," *Microwave Opt. Technol. Lett.*, vol. 20, pp. 179–183, Feb. 1999.

Robert J. Adams (S'91) was born August 21, 1970, in Green Bay, WI. He received the B.S. degree in electrical engineering from Michigan Technological University, Houghton, in 1993 and the M.S. degree in electrical engineering from Virginia Tech, Blacksburg, in 1995. He is currently pursuing the Ph.D. degree as a Fellow of the Bradley Department of Electrical and Computer Engineering at Virginia Tech.

He is a member of the ElectroMagnetic Interactions Laboratory, Bradley Department of Electrical and Computer Engineering, Virginia Tech. His research interests include microwave remote sensing, wave propagation and scattering, and numerical electromagnetics.

Gary S. Brown (S'61–M'67–SM'81–F'86) was born in Jackson, MS, on April 13, 1940. He received the B.S., M.S., and Ph.D. degrees from the University of Illinois, Urbana-Champaign, Urbana, in 1963, 1964, and 1967, respectively.

From 1963 to 1967, he was a Research Assistant in the Antenna Laboratory, University of Illinois, Urbana-Champaign, where he was involved with direction finding, shaped beam antennas, and millimeter waveguides. While in the U.S. Army Signal Corps (1967–1969) he served in an engineering capacity dealing with the integrated wideband communications system (IWCS) in the Republic of Vietnam. During 1970, he was employed by TRW Systems Group, Redondo Beach, CA, where his work involved monopulse, electronic counter measures, and multiple-beam antenna analysis and development. From 1971 to 1973 he was with the Research Triangle Institute, Durham, NC, where his primary area of interest was radar altimetry. From 1973 to 1985 he was employed by Applied Science Associates, Inc., Apex, NC, where he worked with microwave remote sensing, rough surface scattering, and propagation through random media. In 1985, he joined the faculty of Virginia Polytechnic Institute and State University, Blacksburg, VA, where he currently teaches.

Dr. Brown is the Secretary and a member of Commissions B and F of USNC-URSI and he was President of the IEEE Antennas and Propagation Society in 1988. He received the R.W.P. King Award from the Society in 1978. He is presently Director of the ElectroMagnetic Interactions Laboratory at Virginia Tech.